Vol. 632: 145–158, 2019
https://doi.org/10.3354/meps13148

MARINE ECOLOGY PROGRESS SERIES
Mar Ecol Prog Ser

Published December 12

Novel applications of animal-borne Crittercams reveal thermocline feeding in two species of manta ray

Joshua D. Stewart[1,2,*], Taylor R. Smith[1,3], Greg Marshall[4,5], Kyler Abernathy[6], Iliana A. Fonseca-Ponce[7,8,9], Niv Froman[2,10], Guy M. W. Stevens[2]

[1]Scripps Institution of Oceanography, La Jolla, CA 92037, USA
[2]The Manta Trust, Catemwood House, Norwood Lane, Dorset DT2 0NT, UK
[3]Department of Biological Sciences, California State University – Long Beach, Long Beach, CA 90840, USA
[4]National Geographic Remote Imaging Program, Washington, DC 20036, USA
[5]Marshall Innovation LLC, Alexandria, VA 22307, USA
[6]National Geographic Exploration Technology Lab, Washington, DC 20036, USA
[7]Instituto Tecnologico de Bahia de Banderas, Nayarit 63734, Mexico
[8]Instituto Politécnico Nacional, Centro Interdisciplinario de Ciencias Marinas (CICIMAR-IPN), Av. IPN s/n, Colonia Playa Palo de Santa Rita, C.P. 23096 La Paz, Baja California Sur, Mexico
[9]Proyecto Manta Pacific Mexico, Circuito Santa Barbara 88, Rincón del cielo 63735, Bahía de Banderas, Nayarit, Mexico
[10]Department of Veterinary Medicine, University of Cambridge, Cambridge CB3 OES, UK

ABSTRACT: Many marine species rely on oceanographic processes to aggregate prey sources and facilitate feeding opportunities. Numerous studies have demonstrated the importance of oceanographic fronts in the movement and foraging ecology of both predatory and filter feeding marine species. Fewer studies have investigated the importance of vertical pycnoclines (e.g. thermoclines) as foraging queues and prey aggregators. Manta rays, large batoid filter feeders, are believed to rely heavily on mesopelagic and non-surface associated zooplankton prey based on telemetry data, stomach contents, stable isotope, and fatty acid analyses. However, few direct observations exist of non-surface feeding in manta rays. We developed minimally-invasive attachment methods for animal-borne video cameras ('Crittercams') on 2 species of manta ray in Mexico and the Maldives, with the objective of capturing feeding behavior at depth. We achieved retention times of up to 4 h using an active suction attachment with a sealant in oceanic manta rays, and up to 5 h using a J-hook attachment on the upper jaw of reef manta rays. We observed feeding by both species on high-density zooplankton prey that was associated with the thermocline, suggesting that this prey aggregator may be important to the foraging ecology of both species. However, we also captured a variety of social and non-feeding behaviors that occurred within the thermocline, suggesting that telemetry-based temperature and depth data alone cannot facilitate an evaluation of the relative importance of thermocline-associated feeding. We analyzed the impact of different attachment methods on camera retention time, and discuss other relevant applications of these minimally-invasive attachment methods.

KEY WORDS: *Mobula birostris* · *Mobula alfredi* · Mexico · Maldives · Mobulid · Feeding ecology

1. INTRODUCTION

Patchiness is a fundamental characteristic of marine communities that shapes marine species' behaviors, distributions, and foraging strategies (MacArthur & Pianka 1966). Unequal availability of nutrients and light leads to both spatial and temporal heterogeneity in the presence and abundance of primary producers. This in turn leads to patchy distributions of the zooplankton grazers and predators that make up the base of many marine food webs (Blackburn et al. 1970, Longhurst 1976, Sameoto 1986). Coping with patchiness in prey availability is a challenge that many marine species face, and there are numerous

*Corresponding author: josh@mantatrust.org

behavioral adaptations designed to maximize foraging success in the face of patchiness. Search patterns that maximize efficiency in patchy conditions when prey location is unknown, such as Brownian and Lévy walks, are observed across a wide range of taxa (Benhamou 2007). Many marine species associate with oceanographic features that promote productivity and aggregate prey species, such as fronts, in order to use the processes that drive patchiness to their advantage (Sims et al. 2006, Rohner et al. 2014, Scales et al. 2014).

One physical feature that has received less attention for its role in marine patchiness as a prey aggregator is the ubiquitous thermocline. Similar to frontal systems, thermoclines are density boundaries between water masses of different temperatures. These vertical pycnoclines obstruct the passive diffusion of primary producers, creating high concentrations of phytoplankton that attract high densities of grazing zooplankton (Herman 1983, Sameoto 1984, 1986). Telemetry studies have found associations between predatory marine species and thermoclines in some cases, suggesting that fishes, squid, and other larger prey species may also be found in close proximity to the thermocline, perhaps as a result of temperature preferences or oxygen limitations associated with vertical density boundaries (Boyd & Arnbom 1991, Pelletier et al. 2012, Nordstrom et al. 2013).

Filter feeders are often direct consumers of the zooplankton species that are associated with density boundaries. Many studies have demonstrated the link between marine filter feeder movements and frontal systems, highlighting the importance of these oceanographic features to their ecology (Jaine et al. 2014, Scales et al. 2014, Miller et al. 2015). The ability to identify and target dense patches of prey may be especially important to filter feeders, as low prey densities may render feeding energetically unprofitable (Sims 1999, Armstrong et al. 2016). While oceanographic fronts appear to be important features that create foraging opportunities for both filter feeding and predatory species, few studies have examined foraging behavior associated with the thermocline (Pelletier et al. 2012, Nordstrom et al. 2013).

Stewart et al. (2016) found a strong association with the thermocline in oceanic manta rays *Mobula birostris*, which in some cases spent more than 20% of their time per day within or adjacent to the thermocline. As with many telemetry studies, feeding behavior was inferred due to the considerable time spent in proximity to these features and a presumed increase in zooplankton density typically associated with thermoclines. A number of additional studies have found evidence of reliance on non-surface associated zooplankton in both oceanic manta rays (Burgess et al. 2016, Rohner et al. 2017, Stewart et al. 2017a) and closely related reef manta rays *M. alfredi* (Couturier et al. 2013). However, evidence of non-surface feeding is rarely observed directly, and most of these conclusions were drawn from molecular methods such as isotope and fatty acid analysis (Couturier et al. 2013, Burgess et al. 2016, Stewart et al. 2017a), or archival depth and temperature data (Braun et al. 2014, Stewart et al. 2016).

Observing marine species away from accessible coastal sites and below SCUBA diving depths is a persistent challenge in marine ecology. Over the past 3 decades, imaging technology has improved and become small enough to make animal-borne video deployments feasible (Marshall et al. 2007, Moll et al. 2007). Here, we describe a novel, minimally-invasive application of animal-borne video cameras ('Crittercams') with integrated depth and temperature data loggers (Marshall et al. 2007) in both species of manta rays. Our main objective was to directly observe and characterize the thermocline-associated feeding behavior that has been suggested in previous studies. In addition, we discuss the success of different attachment methods as well as research applications outside of foraging studies.

2. MATERIALS AND METHODS

2.1. Study sites

We deployed Crittercams on oceanic manta rays at the Revillagigedo Islands, Mexico (San Benedicto and Socorro Islands), and along the southern coast of Bahia de Banderas, Mexico. We deployed Crittercams on reef manta rays along the eastern edge of Raa Atoll in the Maldives.

The Revillagigedo archipelago is made up of 4 volcanic islands situated 400 km southwest of the Baja California peninsula (at approximately 19° N, 111.5° W). Oceanic manta rays have occasionally been observed ram-feeding on surface zooplankton at these islands (R. Rubin pers. comm., G. Stevens pers. obs.), and submersible dives have revealed manta rays feeding on mesopelagic zooplankton (Stewart et al. 2016). However, manta rays appear to primarily visit the islands to access cleaning stations and socialize with conspecifics (J. Stewart & G. Stevens pers. obs.). Manta rays are found at the Revillagigedo Islands year-round, although manta ray visitation to the islands appears to decrease dur-

ing the summer and autumn months based on acoustic tagging data (R. Rubin pers. comm.). We deployed Crittercams during an 8 d National Geographic research cruise to the Revillagigedo Islands in December 2015.

The southern coast of Bahia de Banderas is characterized by an extremely deep (2000+ m) canyon that comes within 7 km of shore. This high-relief bathymetry creates a productive seasonal upwelling system (Carriquiry et al. 2001) that attracts humpback whales *Megaptera novaeangliae*, a variety of tuna species (*Thunnus* spp.), and oceanic manta rays. Manta rays can be found in the bay mainly during the spring and early summer months, although they are also seen sporadically in the autumn and winter months (I. Fonseca-Ponce & J. Stewart unpubl.). Despite being present during months when surface zooplankton is abundant, manta rays are rarely observed feeding on zooplankton at the surface, and are typically seen transiting along the southern coast within 500 m of shore, or basking at the surface (I. Fonseca-Ponce & J. Stewart pers. obs.). We deployed Crittercams along the southern coast in close proximity to the community of Yelapa (20.49° N, 105.45° W) during two 2 wk field expeditions in March 2016 and March 2017.

Raa Atoll is 1 of 26 geographical atolls that constitute the Maldives archipelago. Located in the north of the country, approximately 150 km from the capital city of Malé, the atoll spans 56 km from north to south (5° 58′ to 5° 20′ N) and 24 km across at its widest (72° 47′ to 73° 02′ E), covering an area of 1180 km^2. Inside the atoll's lagoon, the seabed ranges on average between 40 and 50 m, while outside the channels, the depth drops rapidly to 350 m within 1 km of the atoll's eastern rim. Seasonally reversing monsoonal currents create localized upwelling events, shifting productivity hotspots to the down-current side of the archipelago with each change of the monsoon. Large mobile planktivores, such as reef manta rays, migrate with this shifting productivity and consequently are concentrated in greater numbers on the eastern side of Raa Atoll between the months of May and November during the Southwest monsoon (Anderson et al. 2011). We deployed Crittercams at cleaning stations around Raa Atoll during a 1 wk field expedition in October 2016. These cleaning sites serve as focal areas for social behavior, such as courtship and mating (Stevens et al. 2018). When strong currents flow through to atoll channels, manta rays frequently depart from cleaning stations to feed on the dense zooplankton prey that becomes concentrated at the surface in nearby channels (Stevens 2016).

2.2. Crittercam deployments

The Crittercam platform collects high-resolution (1280 × 720 pixels, 30 frames s^{-1}) video and has an onboard Star-Oddi DST milli-TD temperature and depth recorder set to log temperature every 15 s and depth every 5 s. For deployments on oceanic manta rays in Mexico, we used a suction cup attachment that has previously been used on cetaceans (Fig. 1a). The attachment device is made up of a ca. 20 cm (8 inch) diameter suction cup with circular ridges that reduce the evacuation volume and improve grip. A 1-way valve is mounted through the center of the cup, and an actuator activated at a pre-programmed time by the Crittercam microprocessor dislodges a ball-bearing seal to release the cup for recovery. Active releases were programmed for 17:00 h local time to facilitate recovery before dark. In addition, a zinc-coated steel bolt pierces the suction cup and is secured with a magnesium nut. When immersed in salt water, a galvanic reaction between the 2 metals causes the magnesium nut to dissolve over a roughly predictable duration, loosening the seal formed by the bolt head and causing the suction to release. This serves as an approximately 8 h duration backup release in case the electronic release fails. Crittercams were outfitted with a VHF radio transmitter with an approximately 8 km line-of-sight range that facilitated recovery of cameras after they released from an animal. At the Revillagigedo Islands, we made all deployments by hand, pushing the suction cup firmly onto the rigid dorsal surface between the cephalic fins (Fig. 1b; Supplemental Video S1; www.int-res.com/articles/suppl/m632p145_supp/).

For deployments in Bahia de Banderas in March 2016, we developed an active suction system designed to increase suction force and improve camera deployment times. The active suction system employed a Venturi suction generator that was piped into the suction cup's 1-way valve and driven by pressurized air from a 13 l scuba tank worn by the researcher deploying the camera (Fig. 1c, Video S2). Elasmobranch denticles, the rough tooth-like structures on their skin, create an imperfect attachment surface for the suction cups. Additionally, repeated deployments of the suction cups on the manta rays' skin abraded the smooth surface of the cup, further compromising the seal. While the cups were able to maintain suction for extended periods, perhaps due to the mucus layer on the manta rays' skin, we hypothesized that a sealant could help maintain suction and improve retention times. We tested several potential non-toxic sealants, including sili-

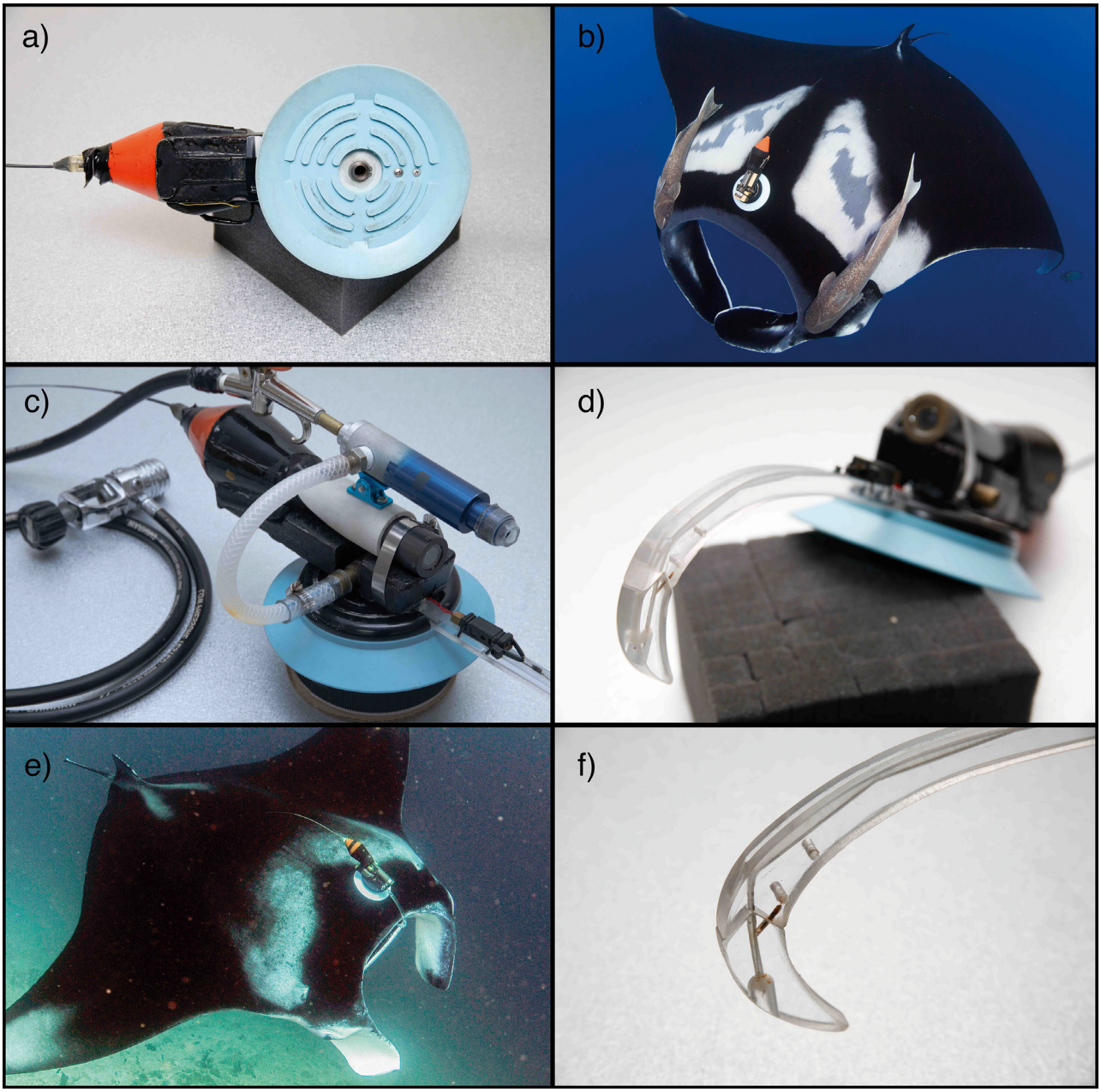

Fig. 1. Crittercam deployments and attachment types. (a) Suction cup attachment used for passive suction attachments, active suction attachments, and for ballast and stability in hook attachments. (b) Crittercam deployed on an oceanic manta ray at the Revillagigedo Islands using passive suction. (c) Venturi active suction system used for active suction deployments. The blue cylinder is the Venturi pump, which creates suction as medium-pressure air is pumped through it from the air gun (silver, extending left from the Venturi pump). (d) J-hook attachment, which loops over the upper jaw and is held in place by forward motion. (e) Crittercam deployed on a reef manta ray in the Maldives using a J-hook attachment. (f) V-shaped break point at the apex of the J-hook, with tension cables to maintain the hook shape until the pre-programmed release time

cone grease, denture cream, and creamy peanut butter.

Suction cups were able to maintain suction on reef manta rays in the Maldives, but they were usually not able to maintain their position for more than a few seconds, quickly sliding off the trailing edge of the pectoral fin. This sliding was perhaps due to the smaller dermal denticles on reef manta rays and the consequent reduced surface friction (Marshall et al. 2009). To resolve this issue, we developed an alternate attachment method that used a J-shaped Plexiglas hook approximately 2 cm wide with a blunt tip to

prevent any puncture injury to the animal (Fig. 1d; Video S3). We placed the hook over the upper jaw, and the camera was held in place passively by the water flow generated by the manta rays' constant forward motion. We attempted 1 deployment with the J-hook alone on a Crittercam without a suction cup attachment, but the reduced mass caused the camera to float upwards and disengage the hook if the manta ray slowed even momentarily. Consequently, all further deployments were made with both the J-hook and the suction cup, which provided mass and stability (Fig. 1e). It is possible that the suction cup also adhered to the dorsal surface of the manta ray, but we suspect that the majority of the camera retention was due to the J-hook, whereas the mass of the suction cup base allowed the hook to remain engaged even at slow swimming speeds. To provide a detachment mechanism, the hook was separated into 2 pieces that joined at the apex of the curve with a V-shaped joint (to prevent swiveling) held together by a galvanically reactive nut and bolt combination with an approximate dissolution time of 8 h. There was no active release on the J-hook as it was crafted in the field. We made deployments using 2 different length hooks, one of 24 cm ('short hook') and one of 28 cm ('long hook').

Due to the success of the J-hook/suction cup combination in the Maldives, we implemented this attachment method on oceanic manta rays in Bahia de Banderas in March 2017. The updated J-hook design also had a V-shaped break point at the apex of the J-hook, although in this case the 2 pieces were held together by a tensioned cable. The tension link passed through a cutting device that could be activated by the Crittercam to facilitate a programmed release (Fig. 1f). We used hooks of 28 cm ('long hook') and 33 cm length ('x-long hook').

To evaluate differences in retention time between attachment methods, we used a time-to-failure Weibull regression (Kalbfleisch & Prentice 2011) using the 'Survival' package in R (Therneau 2011). We considered passive suction, active suction, active suction with a sealant, short hooks, and long hooks as attachment methods, and used models both with and without a sex effect on retention time. We grouped the single passive suction deployment using a sealant with passive suction deployments that did not employ a sealant, as the retention times were very similar. We grouped the x-long hook attachment with long hook attachments. We excluded from statistical analyses the 2 active and passive suction deployments on reef manta rays as they were unsuccessful and not indicative of the retention potential of suction attachments in oceanic manta rays. For the same reason, we excluded 1 short-hook deployment that was terminated early due to a breach by the manta ray, and the single long-hook deployment without a suction cup that quickly detached. We included 2 active suction deployments that were cut short after 3+ h due to scheduled detachments, although these deployments would likely have lasted significantly longer and therefore may underestimate the retention potential of active suction deployments.

For oceanic manta rays, we characterized feeding periods as increased particle (presumably zooplankton) density in the video, unrolled cephalic fins, and increased speed of particulates flowing past the camera for sustained durations. Feeding was more confidently confirmed in reef manta rays as, in addition to unrolled cephalic fins, increased particle density, and increased particle flow, individuals were observed feeding in groups. As a result, individuals feeding near the Crittercam-outfitted manta ray could be seen with open mouths and gill slits, expanded buccal cavities, and undertaking feeding strategy behaviors such as somersault feeding (Stevens 2016). We also classified a 'testing' behavior, where nearby individuals would unroll cephalic fins, swim through a relatively dense patch of particles (presumably zooplankton), and then quickly abort, closing their mouths and gill slits and rolling up the cephalic fins.

2.3. Thermocline analysis

At all 3 study sites, the thermocline extends for several hundred vertical meters (Fig. 2). None of the manta rays outfitted with Crittercams sampled the entire vertical extent of the thermocline, making it impossible to empirically identify the bottom boundary of the thermocline for each deployment. We therefore considered any depth below the mixed layer as being within the thermocline. For each deployment, we created a vertical water column temperature profile by calculating the average temperature at every 1 m depth interval (e.g. Fig. 3b,d,f). We considered the deployment-specific mixed layer depth to be the shallowest depth at which the temperature was 0.5°C less than sea surface temperature recorded during a deployment (Fiedler 2010). We then calculated the proportion of time each manta ray spent within the mixed layer or thermocline, and the proportion of recorded feeding that occurred within the thermocline. For deployments that never reached depths where water temperatures dropped 0.5°C below sea surface temperature, we considered

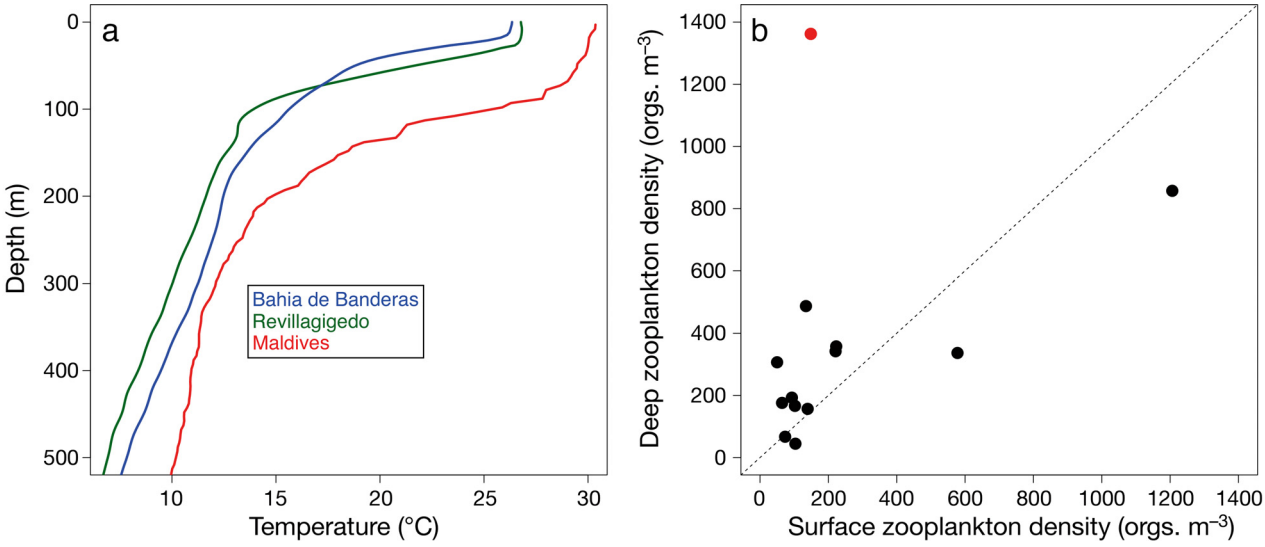

Fig. 2. Thermocline profiles and zooplankton densities. (a) Representative depth/temperature profiles of the 3 study sites, generated using CTD cast data from the World Ocean Database (https://www.nodc.noaa.gov/). (b) Zooplankton densities (organisms m^{-3}) from surface (*x*-axis) and oblique (*y*-axis) net tows conducted in Bahia de Banderas from 2016–2018. The red point represents the zooplankton tow conducted on 30 March 2016, 1 d after BDB07 was observed putatively feeding in the thermocline. The dashed diagonal is the 1:1 line along which surface and deep zooplankton densities would be equal

the manta ray to have spent 100% of its time within the mixed layer.

2.4. Zooplankton sampling and analysis

We conducted zooplankton tows in Bahia de Banderas using a 333 µm mesh plankton net with a 30 cm opening. While zooplankton smaller than the 333 µm mesh size may have escaped from plankton tows, we selected this size based on the pore sizes observed in oceanic manta ray filter plates (approximately 1 mm diameter, with the ability to capture particles smaller than the pore size; Paig-Tran et al. 2013) and the generally large zooplankton prey (e.g. euphausiids) found in studies of oceanic manta ray stomach contents (Rohner et al. 2017). We conducted 10 min plankton tows at speeds of 2–5 knots and used a General Oceanics 2030R flow meter with a standard rotor (rated 0.2–15 knots) to measure the volume of water filtered in each tow. For surface tows, we used a 15 m line to tow the net at the surface in wide circles. For oblique tows, we attached a 2 kg weight to the mouth of the net and lowered the net to depth using a 90 m line. We then maintained an approximately 45° angle between the surface of the water and the line in order to keep the net at 20–45 m depth while towing it in wide circles. We initially used a DiveNav TechBuddy depth recorder to verify that the oblique tows were reaching the intended depth range. The net did not have a closing mechanism, so oblique samples include a small portion of the sample that was collected during recovery to the surface.

We stored all zooplankton samples in 95% ethanol. To analyze the density of organisms in each tow, we first took a subsample of each tow. We diluted the entire sample to 100 ml total volume using 95% ethanol, mixed the sample thoroughly, and used a Hensel-Stempel pipette to extract a 10 ml subsample. We then separated individual organisms into 25 different taxonomic groups following Todd et al. (1996). For each subsample, we counted the number of organisms in each group and multiplied that by 10 to account for the total sample volume. We used a paired *t*-test to evaluate differences between plankton densities in surface versus oblique plankton tows.

3. RESULTS

We made a total of 12 Crittercam deployments on oceanic manta rays at the Revillagigedo Islands in December 2015 using passive suction hand deployments (Table 1). The deployments lasted a mean ± SD of 78.9 ± 43.21 min (range 19.5–171 min), and in all but 2 cases the cameras detached when the passive suction was no longer adequate, as opposed to releasing at the scheduled deployment end time. Camera-tagged manta rays interacted with both conspecifics and SCUBA divers at cleaning stations and

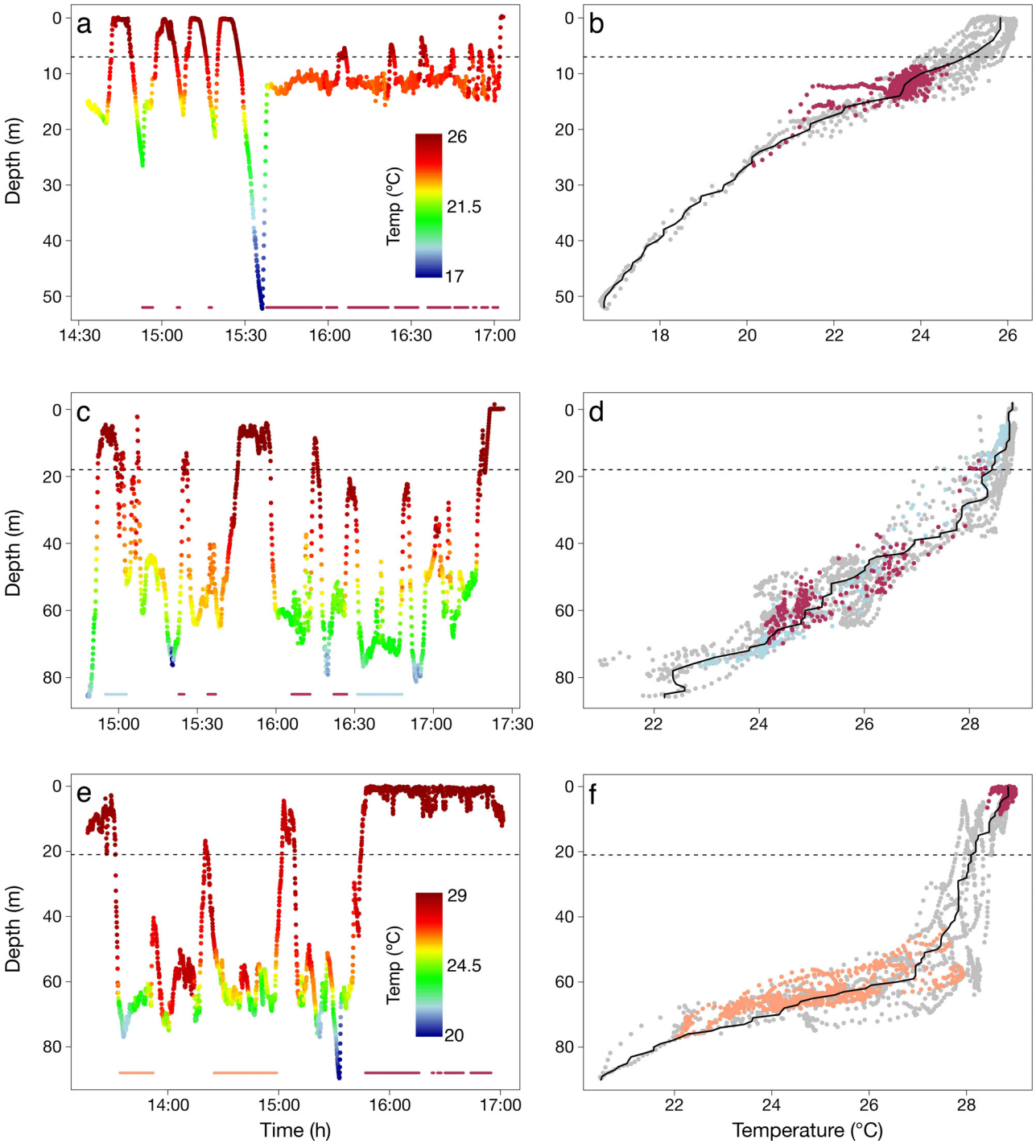

Fig. 3. Dive profiles of manta rays observed feeding using Crittercams (left column) and depth-temperature profiles recorded during Crittercam deployments (right column): (a,b) oceanic manta ray in Bahia de Banderas (BDB07); (c,d) reef manta ray MDV16 and (e,f) reef manta ray MDV09, both in the Maldives. Panels a, c, and e are depth time series, with colors representing water temperature. The temperature legend in e also applies to c. Points along the bottom of a, c, and e represent behaviors recorded by Crittercams. Red points are feeding, blue points are testing, and orange points are courtship behavior (see Section 2.2 for descriptions of these behaviors). These correspond to the points of the same colors in panels b, d, and f (gray points: all other behaviours, e.g. cruising, cleaning). Panels b, d, and f are vertical profiles of the water column (depth and temperature) created from the corresponding time series in a, c, and e. Black lines represent the smoothed average temperature at each depth in 1 m increments. Horizontal dashed lines represent the deployment-specific mixed layer depth (see Section 2.3 for details). Any depths below the mixed layer were considered to be within the thermocline

Table 1. Crittercam deployments on manta rays in Mexico and the Maldives. Deployment durations are rounded to the nearest quarter minute. (–) indicates camera was not shed and no breach or other shedding attempt was made. NA: data not available due to temperature/depth recorder failures. Dates are given as mo/d/yr

ID	Sex	Deployment location	Deployment date	Attachment	Sealant	Deployment duration (min)	Camera shed	Released on schedule	% Time in thermocline	% Time foraging	% Foraging in thermocline
REV01	M	Revillagigedo Islands	12/3/15	Passive suction	N	20.75	–	N	0.00	0.00	0.00
REV02	M	Revillagigedo Islands	12/3/15	Passive suction	N	58.25	–	N	33.59	0.00	0.00
REV03	F	Revillagigedo Islands	12/4/15	Passive suction	N	118.50	–	N	28.05	0.00	0.00
REV04	F	Revillagigedo Islands	12/4/15	Passive suction	N	89.25	–	Y	0.00	0.00	0.00
REV05	F	Revillagigedo Islands	12/6/15	Passive suction	N	57.00	–	N	0.00	0.00	0.00
REV06	M	Revillagigedo Islands	12/7/15	Passive suction	N	19.50	–	N	0.00	0.00	0.00
REV07	M	Revillagigedo Islands	12/7/15	Passive suction	N	62.50	–	N	94.79	0.00	0.00
REV08	M	Revillagigedo Islands	12/7/15	Passive suction	N	50.50	–	N	88.93	0.00	0.00
REV09	M	Revillagigedo Islands	12/8/15	Passive suction	N	100.00	–	N	NA	0.00	0.00
REV10	F	Revillagigedo Islands	12/8/15	Passive suction	N	91.00	–	N	0.00	0.00	0.00
REV11	F	Revillagigedo Islands	12/8/15	Passive suction	N	171.00	–	N	7.44	0.00	0.00
REV12	M	Revillagigedo Islands	12/8/15	Passive suction	N	109.00	–	Y	NA	0.00	0.00
BDB01	?	Bahia de Banderas	3/23/16	Active suction	N	57.75	–	N	86.26	0.00	0.00
BDB02	?	Bahia de Banderas	3/23/16	Active suction	N	91.50	–	N	48.34	0.00	0.00
BDB03	F	Bahia de Banderas	3/28/16	Active suction	N	226.50	–	Y	45.69	0.00	0.00
BDB04	?	Bahia de Banderas	3/28/16	Active suction	N	134.75	–	N	28.46	0.00	0.00
BDB05	F	Bahia de Banderas	3/29/16	Active suction	N	27.50	–	N	30.08	0.00	0.00
BDB06	F	Bahia de Banderas	3/29/16	Active suction	Y	22.50	–	N	44.08	0.00	0.00
BDB07	F	Bahia de Banderas	3/29/16	Active suction	Y	240.50	–	Y	51.39	29.29	100.00
BDB08	?	Bahia de Banderas	3/29/16	Active suction	Y	67.50	–	N	25.27	0.00	0.00
BDB09	F	Bahia de Banderas	3/30/16	Passive suction	Y	70.00	–	N	36.14	0.00	0.00
BDB10	F	Bahia de Banderas	3/31/16	Active suction	Y	224.00	–	N	38.46	0.00	0.00
MDV01	F	Maldives	10/7/16	Active suction	N	14.50	–	N	58.57	0.00	0.00
MDV02	F	Maldives	10/10/16	Short hook	N	156.25	–	N	67.36	0.00	0.00
MDV03	?	Maldives	10/10/16	Passive suction	N	2.75	–	N	0.00	0.00	0.00
MDV04	F	Maldives	10/11/16	Short hook	N	33.25	–	N	0.00	0.00	0.00
MDV05	F	Maldives	10/11/16	Long hook	N	36.00	–	N	0.00	0.00	0.00
MDV06	F	Maldives	10/11/16	Long hook (no suction cup)	N	4.25	–	N	0.00	0.00	0.00
MDV07	F	Maldives	10/11/16	Short hook	N	40.50	–	N	10.38	0.00	0.00
MDV08	M	Maldives	10/11/16	Long hook	N	48.25	–	N	91.00	0.00	0.00
MDV09	F	Maldives	10/11/16	Long hook	N	250.50	–	N	55.08	21.32	0.00
MDV10	F	Maldives	10/11/16	Short hook	N	44.00	–	N	91.82	0.00	0.00
MDV11	F	Maldives	10/12/16	Long hook	N	176.00	–	N	60.22	0.00	0.00
MDV12	F	Maldives	10/12/16	Short Hook	N	32.25	–	N	17.05	0.00	0.00
MDV13	M	Maldives	10/12/16	Short Hook	N	61.00	–	N	56.55	0.00	0.00
MDV14	F	Maldives	10/12/16	Short Hook	N	6.00	Breach	N	0.00	0.00	0.00
MDV15	M	Maldives	10/12/16	Long Hook	N	302.50	Breach	N	50.74	0.00	0.00
MDV16	?	Maldives	10/12/16	Short Hook	N	196.50	Breach[a]	N	83.20	8.82	97.11
BDB11	F	Bahia de Banderas	3/24/17	X-Long Hook	N	119.50	–	N	9.14	0.00	0.00
BDB12	M	Bahia de Banderas	3/24/17	Long Hook	N	148.50	Breach	N	35.84	0.00	0.00

[a]Indicates a breach where the camera was not shed by the manta

in pelagic and near-shore environments, as detailed by Stewart et al. (2017b). We did not record any feeding events at the Revillagigedo Islands. Social behaviors by oceanic manta rays in the Revillagigedo Islands recorded during Crittercam deployments are reported by Stewart et al. (2017b).

We made a total of 10 Crittercam deployments in Bahia de Banderas in March 2016. One of these was made with a passive hand deployment and a sealant, 5 with the active suction Venturi pump, and 4 with active suction and a sealant (Table 1). Of all the sealants we tested, only creamy peanut butter was sufficiently viscous to remain applied to the suction cup upon entry to the water, and while swimming for an extended period to reach the study subject. Other candidate sealants quickly dissolved in seawater. All reported deployments with a sealant used creamy peanut butter. The passive suction deployment with sealant lasted 70 min, active suction deployments (n = 5) lasted a mean of 107.6 ± 77.51 min (range 27.5–226.5 min), and active suction deployments with sealant (n = 4) lasted 138.6 ± 109.87 min (range 22.5–240.5 min). Two deployments lasted until planned release times, while the remaining 8 deployments detached prematurely. Active suction deployments frequently left a white marking in the shape of the suction cup on the dorsal surface of the manta rays (Fig. A1 in the Appendix). Pigment cells are embedded in the mucus layer on the dorsal surface (Kashiwagi et al. 2015), and were likely removed along with a ring of mucus at the attachment site of the suction cups. In some cases, manta rays with these suction cup markings were resighted 2 to 3 d after deployment, and the markings had faded to a barely visible grey ring, suggesting that these impacts are not long lasting. In some cases, manta rays swam away rapidly after deployments, but returned to normal behavior 20–90 s later. Differences in reactions to various attachment types and between species, and the impacts of these reactions on analyses of social and other behaviors are currently being assessed (N. Pelletier et al. unpubl.). Short-duration changes in behavior in response to camera deployment did not coincide with or affect our evaluations of feeding behavior.

We captured Crittercam footage of 1 oceanic manta ray (BDB07) feeding between 10 and 20 m depth in the thermocline for a total of 70.75 min (Fig. 3a,b; Video S4) on 29 March 2016. The Crittercam detached and was recovered approximately 500 m from shore, in contrast to the ~100 m coastal band where manta rays are typically observed in the region. During the 20 min period that we were searching for and retrieving the Crittercam, we encountered 5 manta rays at the surface between 300 and 500 m offshore in proximity to the Crittercam recovery location. Due to the unusually high density of manta rays at the recovery location, and review of the video that suggested feeding behavior, we returned to the recovery location the following morning (30 March 2016) to conduct plankton tows. A 10 min surface plankton tow revealed a zooplankton density of 148.5 organisms m^{-3}, comprised primarily of radiolarians (39.2%) and copepods (23.6%). A 10 min oblique plankton tow made between 10 and 20 m depth revealed a zooplankton density of 1362 organisms m^{-3}, nearly 10 times higher than the paired surface tow, comprised primarily of ostracods (56.2%) and copepods (32.7%). In contrast, 11 subsequent paired surface and oblique tows performed between April 2017 and February 2018 revealed a mean ± SD density of 249.05 ± 333.41 organisms m^{-3} at the surface and 290.85 ± 220.69 organisms m^{-3} at depth. We found no statistically significant difference between densities of surface and oblique zooplankton tows ($p = 0.227$). Surface zooplankton tows were made up of primarily copepods (55.77%), cladocerans (25.85%), fish eggs (5.7%), and ostracods (3.81%). Oblique zooplankton tows were made up of primarily copepods (60%), cladocerans (26.84%), chaetognaths (3.15%), and ostracods (2.99%).

We made a total of 16 Crittercam deployments on reef manta rays in Raa Atoll during 7–12 November 2016. One deployment using active suction lasted 14.45 min before sliding off the trailing edge of the manta ray's pectoral fin. One deployment using passive suction lasted 2.75 min. The single deployment using only a hook attachment with no suction cup lasted 4.25 min. Two manta rays shed cameras by breaching, one after 6 min and the other after 301 min. Excluding the manta ray that shed its camera after 6 min (as this is not indicative of retention potential), deployments using the short hook (n = 7) lasted a mean ± SD of 80.53 ± 48.01 min (range 32.25–196.5 min). Deployments using the long hook (n = 5; excluding the 4.25 min deployment with no suction cup) lasted a mean of 162.65 ± 118.32 min (range 36–302.5 min).

We observed 2 feeding events by reef manta rays outfitted with Crittercams. One deployment, MDV16 on 12 October 2016, captured feeding behavior in the thermocline between 20 and 70 m depth for a total of 17.25 min (Fig. 3c,d; Video S5). The second feeding manta ray, MDV09 on 11 October 2016, was recorded swimming with unrolled cephalic fins (and presumably feeding) at the surface for a total of 53.5 min with a large group of other reef manta rays feeding in

a shallow channel between islands. This individual and many other reef manta rays outfitted with Crittercams were recorded engaging in courtship behavior (as defined by Stevens et al. 2018) in the thermocline between 50 and 80 m depth (Fig. 3e,f; N. Pelletier et al. unpubl.).

In March 2017, oceanic manta rays in Bahia de Banderas were distributed in the center of the bay over deep water, as opposed to their typical distribution close to shore in shallow water. As a result, individuals were much more challenging to work with, and we successfully conducted only 2 Crittercam deployments using the updated hook attachment with an active release. The deployments lasted 119.5 (x-long hook) and 148.5 min (long hook), and both detached prior to the scheduled release times. BDB12 shed its camera by breaching at 148.5 min. No feeding behavior was observed in either deployment.

Despite differences in the mean retention time among attachment methods (Fig. 4), the time-to-failure Weibull regression found no statistically significant differences between attachment methods ($p > 0.2$ in all cases). There was no statistically significant effect of sex on retention time ($p = 0.267$). The long hook attachment method (n = 7, including x-long hook) had the longest retention time (maximum 302.5 min, mean ± SD 154.46 ± 98.47 min) followed by active suction with a sealant (n = 4, max 240.50 min, mean 138.63 ± 109.86 min), active suction with no sealant (n = 5, max 226.50 min, mean 107.60 ± 77.52 min), the short hook (n = 7, max 196.5, mean 80.53 ± 67.17 min), and passive suction (n = 13, max 171.00 min, mean 78.25 ± 41.45 min).

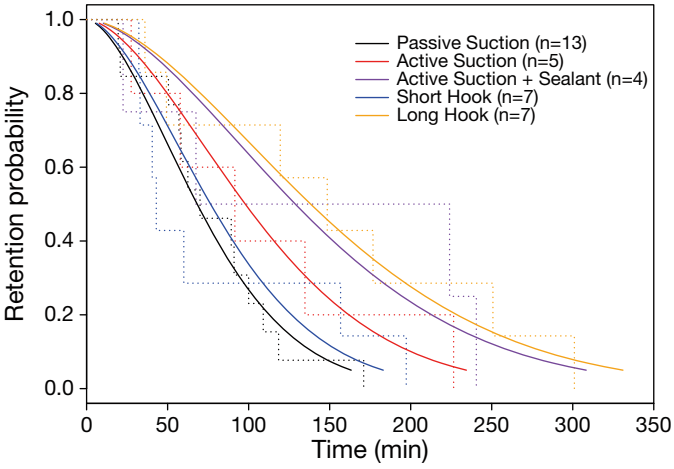

Fig. 4. Weibull regression retention curves for different Crittercam attachment methods. Dotted lines represent the proportion of Crittercams still attached at a given time point. Solid lines represent the modeled retention probability at a given time point

4. DISCUSSION

The animal-borne video data presented here confirm that manta rays forage in the thermocline, taking advantage of physical processes that aggregate their zooplankton prey and, presumably, increase their feeding efficiency. Our zooplankton tow in Bahia de Banderas on the day following the recording of putative feeding demonstrates the effectiveness of the thermocline in concentrating zooplankton, with almost 10 times the density in the oblique tow compared with the surface tow at the same location. However, subsequent zooplankton tows in Bahia de Banderas illustrate the spatial and temporal variability in zooplankton densities in the bay, and further highlight the patchy foraging environment that manta rays and other marine species experience. While the zooplankton tows from 30 March 2016 do not represent the exact conditions that BDB07 encountered on the previous day, the extremely high zooplankton densities at depth compared with the surface provide a plausible explanation for the thermocline feeding behavior captured on video. In the Maldives, MDV16 engaged in feeding behavior primarily between 40 and 70 m within the thermocline, whereas we observed testing behavior (beginning but quickly aborting feeding) by it and adjacent manta rays at the base of the mixed layer (shallower than 20 m) and deeper than 70 m (Fig. 3c,d). This suggests that zooplankton density was highest near the upper boundary of the thermocline where it approaches the mixed layer, creating high-biomass prey patches that are likely essential to supporting the foraging energetics of manta rays and other filter feeders (Sims 1999, Armstrong et al. 2016, Stewart et al. 2017a).

The putative feeding observation in Bahia de Banderas also highlights the potential importance of fine-scale water column dynamics in aggregating prey. In 2 cases, putative feeding occurred along a constant depth while temperatures dropped more than 2°C (Fig. 3b). This may be indicative of complex microstructures created by localized upwelling along the high-relief bathymetry in the area. These microstructures may serve a similar function to thermoclines but on a smaller scale, and may also be important in the foraging dynamics of filter feeders. Previous studies have highlighted the apparent importance of the thermocline to the diving behavior and foraging success of marine predators such as seals and penguins (Boyd & Arnbom 1991, Pelletier et al. 2012, Nordstrom et al. 2013), although these predators were targeting higher trophic level species such as

fishes and squid. The thermocline has long been recognized as an oceanographic feature that can physically shape or limit the distribution of species ranging from zooplankton to tunas (Green 1967, Sameoto 1984, 1986). The present study contributes to a growing body of work demonstrating the importance of the thermocline in facilitating feeding opportunities for a wide range of marine species through these biophysical processes.

While our observations qualitatively demonstrate the potential importance of the thermocline as a foraging cue for manta rays, quantifying the relative importance of different prey communities would require collecting prey data concurrently with manta ray movements and behavioral observations, a logistically challenging proposition (Stewart et al. 2018). Pairing animal-borne cameras with autonomous echo sounders (e.g. Lawson et al. 2015) could potentially facilitate the concurrent collection of behavioral data and zooplankton density. This would open numerous opportunities to explore prey targeting and foraging energetics in manta rays and a wide variety of other marine species. However, in future studies, it will be important to identify new approaches to confirming feeding behavior (e.g. using camera attachments that provide a view of the individual's mouth). While the video footage of BDB07 was presumed to be feeding behavior based on particle density and flow rate, and unrolled cephalic fins, it was only possible to confirm feeding behavior in the Maldives, where conspecifics were visible in the footage. This highlights a challenge to studying feeding behavior with animal-borne video cameras in oceanic manta rays, which appear to spend less time with conspecifics.

Importantly, manta rays were observed engaging in numerous non-feeding behaviors in the thermocline. In particular, courtship behavior resulted in rapid, acrobatic vertical movements in reef manta rays that appear similar to feeding behavior from depth time series (Fig. 1c–f) and would likely be indistinguishable in accelerometer data as well (Videos S5 & S6). This demonstrates the utility of animal-borne videos in characterizing behavior when direct observations are not possible, and highlights the limitations of behavioral interpretations from telemetry data, including both temperature/depth recorders and accelerometers. For example, the 10–20% of oceanic manta rays' time spent in the thermocline reported by Stewart et al. (2016) may or may not have actually been representative of time spent feeding. Manta rays may associate with the thermocline while feeding, but may also spend considerable time swimming within the thermocline searching for opportunities to forage or engage with conspecifics. We encountered only 3 feeding events in over 63 h of video data. This is likely due to deployments occurring primarily at cleaning stations, which are associated with other social behaviors rather than foraging (Stevens et al. 2018). In all 3 cases of feeding (BDB07, MDV09, and MDV16), Crittercam deployments lasted more than 3 h. In the case of the 2 reef manta ray feeding events, this likely gave the animals enough time to depart from the cleaning stations and begin to access habitats more typically associated with foraging. While our limited sample size and feeding observations do not allow us to quantify the frequency of different feeding behaviors, thermocline feeding and channel-associated feeding were both observed once in reef manta rays. Feeding in the channels between atolls is frequently observed in the Maldives (Stevens 2016) but was only captured once by Crittercams, suggesting that thermocline feeding could potentially be a more common strategy than its relative frequency in our results suggests.

In Bahia de Banderas, manta rays are rarely seen feeding or cleaning, despite their high abundance for approximately 6 mo each year (I. Fonseca-Ponce & J. Stewart unpubl.). If manta rays are primarily feeding in the thermocline and on non-surface zooplankton, this would explain the paucity of surface feeding observations in the region. At the Revillagigedo Islands, oceanic manta rays are rarely observed feeding, and divers typically find them socializing at cleaning stations. This, combined with the relatively short passive suction deployments (mean 62.75 min, max 118.5 min), likely explains why no feeding observations were recorded at the islands. Several studies suggest that both species of manta ray visit cleaning stations during the day and access deeper, offshore waters at night to feed (Braun et al. 2014, Stewart et al. 2016, Couturier et al. 2018, Setyawan et al. 2018). Further capturing and characterizing feeding behaviors using animal-borne cameras may require achieving longer deployments, deploying cameras overnight, and using camera packages with a light source or low-light cameras to avoid artificial-light related behavioral changes.

The lack of statistically significant differences in retention time between attachment methods is most likely a combination of small sample sizes and the ubiquity of short (<30 min) deployments across all attachment types. Despite the lack of statistical significance, there appear to be differences among attachment types that can support guidelines for future deployments. Passive suction provided the shortest retention times, and was substantially improved

upon by implementing the Venturi active suction system in oceanic manta rays. While the use of a sealant (i.e. creamy peanut butter) generally appeared to increase retention times, active suction deployments both with and without a sealant achieved similar maximum retention times (240.5 min with sealant and 226.5 min without). We hypothesize that retention differences (and similarities) between these 2 attachment types were due to individual variability in dermal mucus thickness. In 1 case (which was not recorded as a deployment), we deployed a Crittercam with the active suction attachment, and the camera immediately detached from the animal. We attempted a second deployment by hand (passive suction), and the suction cup immediately came loose a second time. Upon close inspection of the animal, there was virtually no mucus on the dorsal surface, which led to the application of a sealant in later deployments. In individuals with a thick dorsal mucus layer, active suction deployments without a sealant would presumably exhibit similarly long retention times as those employing a sealant (e.g. BDB03).

The difference between retention times in short- and long-hook deployments was surprisingly large, with short hooks performing worse than active suction, and long hooks exhibiting the longest retention times of all attachment methods. The long hook may have allowed the Crittercam to sit in a more stable position, particularly when the animals turned and the camera began to slide laterally along the head. In addition to improved retention time, the position of the camera with the long hook attachment provided a better view of the cephalic fins and upper jaw, assisting with interpretation of behaviors such as feeding, courtship, and socialization. While both the hook and suction attachments were minimally invasive, we only observed breaches in hook deployments. In the 4 cases of breaches, manta rays jumped out of the water and somersaulted backwards to land on their dorsal surface, dislodging the Crittercam and terminating the deployment in all but 1 case. We interpret these as attempts to shed the cameras, suggesting that the hook attachment may have been more noticeable or irritating to the manta rays than the suction attachment. Despite these shedding attempts, manta rays with hook attachments engaged in normal cleaning, feeding, courtship, and other social behaviors during Crittercam deployments, suggesting that any influences on animal behavior were minimal. Based on these results, we suggest that future deployments of animal-borne cameras on oceanic manta rays consider either 28+ cm hook attachments or active suction attachments with sealant to maximize retention time, while only hook attachments (ideally 28+ cm) appear to be viable for reef manta rays.

5. CONCLUSION

In this study, animal-borne Crittercams provided new insights into the ecology of both reef and oceanic manta rays. These minimally-invasive, short-term deployments were able to capture several feeding events, confirming that thermocline feeding occurs in both species, as well as numerous social interactions (Stewart et al. 2017b, N. Pelletier et al. unpubl.). The suction and hook attachments employed here could also prove useful for deployments of other instruments such as accelerometers, which need to remain stationary on the study subject. This could be particularly relevant for post-release mortality studies of mobulid rays captured in fisheries, where survival probability can often be evaluated within a few hours following release (Whitney et al. 2016, Francis & Jones 2017). To further evaluate feeding behavior in mobulid rays using animal-mounted cameras, we encourage future research targeting crepuscular and nighttime periods, which would require further refinement and use of on-board light sources. In addition, longer deployment times could be facilitated through traditional tag attachment methods (e.g. subdermal anchors), dorsal fin-mounted towed tags, or temporary harness attachments (Fontes et al. 2018).

Acknowledgements. This research was approved by the UC San Diego Institutional Animal Care and Use Committee (Protocol S12116), and conducted with permission from the relevant authorities in Mexico (Permit SEMARNAT FAUT 0265) and the Maldives (Permits [OTHR]30-D/INDIV/2016/291 and EPA/2016/PSR-M01). This research was supported by a National Geographic Waitt Grant (414-15). We thank Thomas P. Peschak for facilitating a National Geographic research cruise to the Revillagigedo Islands in December 2015. We thank the community members of Yelapa and David Connell for assistance with deployments in Bahia de Banderas, Mexico. The research expedition in the Maldives was made possible thanks to the permission and support provided by the Maldives Ministry of Fisheries and Agriculture and the Ministry of Environment and Energy. We also thank the Four Seasons Resort at Landaa Giraavaru for providing accommodation to the research team while transiting to Raa and for their contribution to the expedition`s logistics.

LITERATURE CITED

Anderson RC, Adam MS, Goes JI (2011) From monsoons to mantas: seasonal distribution of *Manta alfredi* in the Maldives. Fish Oceanogr 20:104–113

Armstrong AO, Armstrong AJ, Jaine FRA, Couturier LIE

and others (2016) Prey density threshold and tidal influence on reef manta ray foraging at an aggregation site on the Great Barrier Reef. PLOS ONE 11:e0153393
Benhamou S (2007) How many animals really do the Levy Walk? Ecology 88:1962–1969
Blackburn M, Laurs RM, Owen RW, Zeiyzschel B (1970) Seasonal and areal changes in standing stocks of phytoplankton, zooplankton and micronekton in the eastern tropical Pacific. Mar Biol 7:14–31
Boyd IL, Arnbom T (1991) Diving behaviour in relation to water temperature in the southern elephant seal: foraging implications. Polar Biol 11:259–266
Braun CD, Skomal GB, Thorrold SR, Berumen ML (2014) Diving behavior of the reef manta ray links coral reefs with adjacent deep pelagic habitats. PLOS ONE 9: e88170
Burgess KB, Couturier LIE, Marshall AD, Richardson AJ, Weeks S, Bennett MB (2016) *Manta birostris*, predator of the deep? Insight into the diet of the giant manta ray through stable isotope analysis. R Soc Open Sci 3:160717
Carriquiry JD, Cupul-Magaña AL, Rodríguez-Zaragoza F, Medina-Rosas P (2001) Coral bleaching and mortality in the Mexican Pacific during the 1997-98 El Niño and prediction from a remote sensing approach. Bull Mar Sci 69: 237–249
Couturier LIE, Rohner CA, Richardson AJ, Marshall AD and others (2013) Stable isotope and signature fatty acid analyses suggest reef manta rays feed on demersal zooplankton. PLOS ONE 8:e77152
Couturier LIE, Newman P, Jaine FRA, Bennett MB and others (2018) Variation in occupancy and habitat use of *Mobula alfredi* at a major aggregation site. Mar Ecol Prog Ser 599:125–145
Fiedler PC (2010) Comparison of objective descriptions of the thermocline. Limnol Oceanogr Methods 8:313–325
Fontes J, Baeyaert J, Prieto R, Graca G, Buyle F, Afonso P (2018) New non-invasive methods for short-term electronic tagging of pelagic sharks and rays. Mar Biol 165:34
Francis MP, Jones EG (2017) Movement, depth distribution and survival of spinetail devilrays (*Mobula japanica*) tagged and released from purse-seine catches in New Zealand. Aquat Conserv 27:219–236
Green RE (1967) Relationship of the thermocline to success of purse seining for tuna. Trans Am Fish Soc 96:126–130
Herman AW (1983) Vertical distribution patterns of copepods, chlorophyll, and production in northeastern Baffin Bay. Limnol Oceanogr 28:709–719
Jaine FRA, Rohner CA, Weeks SJ, Couturier LIE, Bennett MB, Townsend KA, Richardson AJ (2014) Movements and habitat use of reef manta rays off eastern Australia: offshore excursions, deep diving and eddy affinity revealed by satellite telemetry. Mar Ecol Prog Ser 510:73–86
Kalbfleisch JD, Prentice RL (2011) The statistical analysis of failure time data, Vol 360. John Wiley & Sons, Hoboken, NJ
Kashiwagi T, Maxwell EA, Marshall AD, Christensen AB (2015) Evaluating manta ray mucus as an alternative DNA source for population genetics study: underwater-sampling, dry-storage and PCR success. PeerJ 3:e1188
Lawson GL, Hückstädt LA, Lavery AC, Jaffré FM and others (2015) Development of an animal-borne 'sonar tag' for quantifying prey availability: test deployments on northern elephant seals. Anim Biotelem 3:22
Longhurst AR (1976) Interactions between zooplankton and phytoplankton profiles in the eastern tropical Pacific Ocean. Deep-Sea Res Oceanogr Abstr 23:729–754
MacArthur RH, Pianka ER (1966) On optimal use of a patchy environment. Am Nat 100:603–609
Marshall G, Bakhtiari M, Shepard M, Tweedy J III and others (2007) An advanced solid-state animal-borne video and environmental data-logging device (Crittercam) for marine research. Mar Technol Soc J 41:31–38
Marshall AD, Compagno LJV, Bennett MB (2009) Redescription of the genus *Manta* with resurrection of *Manta alfredi*. Zootaxa 2301:1–28
Miller PI, Scales KL, Ingram SN, Southall EJ, Sims DW (2015) Basking sharks and oceanographic fronts: quantifying associations in the north-east Atlantic. Funct Ecol 29:1099–1109
Moll RJ, Millspaugh JJ, Beringer J, Sartwell J, He Z (2007) A new 'view' of ecology and conservation through animal-borne video systems. Trends Ecol Evol 22:660–668
Nordstrom CA, Battaile BC, Cotté C, Trites AW (2013) Foraging habitats of lactating northern fur seals are structured by thermocline depths and submesoscale fronts in the eastern Bering Sea. Deep Sea Res II 88–89:78–96
Paig-Tran EWM, Kleinteich T, Summers AP (2013) The filter pads and filtration mechanisms of the devil rays: variation at macro and microscopic scales. J Morphol 274: 1026–1043
Pelletier L, Kato A, Chiaradia A, Ropert-Coudert Y (2012) Can thermoclines be a cue to prey distribution for marine top predators? A case study with little penguins. PLOS ONE 7:e31768
Rohner CA, Weeks SJ, Richardson AJ, Pierce SJ and others (2014) Oceanographic influences on a global whale shark hotspot in southern Mozambique. PeerJ PrePrints 2:e661v1
Rohner CA, Burgess KB, Rambahiniarison JM, Stewart JD, Ponzo A, Richardson AJ (2017) Mobulid rays feed on euphausiids in the Bohol Sea. R Soc Open Sci 4:161060
Sameoto DD (1984) Vertical distribution of zooplankton biomass and species in northeastern Baffin Bay related to temperature and salinity. Polar Biol 2:213–224
Sameoto DD (1986) Influence of the biological and physical environment on the vertical distribution of mesozooplankton and micronekton in the eastern tropical Pacific. Mar Biol 93:263–279
Scales KL, Miller PI, Hawkes LA, Ingram SN, Sims DW, Votier SC (2014) On the front line: frontal zones as priority at-sea conservation areas for mobile marine vertebrates. J Appl Ecol 51:1575–1583
Setyawan E, Sianipar AB, Erdmann MV, Fischer AM and others (2018) Site fidelity and movement patterns of reef manta rays (*Mobula alfredi*: Mobulidae) using passive acoustic telemetry in northern Raja Ampat, Indonesia. Nat Conserv Res 3:1–15
Sims DW (1999) Threshold foraging behaviour of basking sharks on zooplankton: life on an energetic knife-edge? Proc R Soc B 266:1437–1443
Sims DW, Witt MJ, Richardson AJ, Southall EJ, Metcalfe JD (2006) Encounter success of free-ranging marine predator movements across a dynamic prey landscape. Proc R Soc B 273:1195–1201
Stevens GMW (2016) Conservation and population ecology of manta rays in the Maldives. PhD thesis, University of York
Stevens GMW, Hawkins JP, Roberts CM (2018) Courtship and mating behaviour of manta rays *Mobula alfredi* and *M. birostris* in the Maldives. J Fish Biol
Stewart JD, Jaine FRA, Armstrong AJ, Armstrong AO and others (2018) Research priorities to support effective manta and devil ray conservation. Front Mar Sci 5:314

Stewart JD, Hoyos-Padilla EM, Kumli KR, Rubin RD (2016) Deep-water feeding and behavioral plasticity in *Manta birostris* revealed by archival tags and submersible observations. Zoology 119:406–413

Stewart JD, Rohner CA, Araujo G, Avila J and others (2017a) Trophic overlap in mobulid rays: insights from stable isotope analysis. Mar Ecol Prog Ser 580:131–151

Stewart JD, Stevens GMW, Marshall GJ, Abernathy K (2017b) Are mantas self aware or simply social? A response to Ari and D'Agostino 2016. J Ethol 35:145–147

Therneau TM (2011) A package for survival analysis in S. version 2.38. https://CRAN.R-project.org/package=survival

Todd CD, Laverack MS, Boxshall G (1996) Coastal marine zooplankton: a practical manual for students, 2nd edn. Cambridge University Press, Cambridge

Whitney NM, White CF, Gleiss AC, Schwieterman GD, Anderson P, Hueter RE, Skomal GB (2016) A novel method for determining post-release mortality, behavior, and recovery period using acceleration data loggers. Fish Res 183:210–221

Appendix.

Fig. A1. Markings left by active suction attachment on an oceanic manta ray in Bahia de Banderas, Mexico

Editorial responsibility: Elliott Hazen, Pacific Grove, California, USA

Submitted: February 19, 2019; Accepted: September 30, 2019
Proofs received from author(s): November 29, 2019